



Arsenic removal using *Prosopis spicigera* L. wood (PsLw) carbon–iron oxide composite

Ramasubbu DhanaRamalakshmi¹ · Mahalingam Murugan² · Vincent Jeyabal³

Received: 7 January 2020 / Accepted: 24 August 2020 / Published online: 5 September 2020
© The Author(s) 2020

Abstract

The present manuscript reports the removal of arsenic from aqueous solution using iron oxide composite of carbon derived from the plant material *Prosopis spicigera* L. wood which depletes the ground water of ponds, lakes and other water bodies. The adsorbent was characterised by Fourier Transform Infra Red spectroscopy and Scanning Electron Microscope for surface analysis; Brunauer–Emmett–Teller and methylene blue method for surface area determination and pH_{zpc} for surface charge determination. Experimental conditions such as pH, contact time, adsorbate initial concentration and in the presence other ions are varied to study the batch adsorption equilibrium experiment. The adsorption process was tested with Langmuir and Freundlich isotherm model and Langmuir isotherm was best suited. Sorption kinetics was analysed with pseudo-first- and second-order kinetics but adsorption follows second order kinetics. For an initial concentration of 60 mg/L of As(III) ions, adsorption capacity was found to be 83.84 mg/g at $\text{pH}=6.0$. Thermodynamically the adsorption process is spontaneous, feasible and endothermic in nature. Adsorption involves pore diffusion, external mass transfer and complex formation. Column study was performed to apply this process for large scale treatment.

Keywords Adsorption · Arsenic · Isotherm · Kinetics · PsLw carbon · Thomas model

Introduction

The presence of arsenic in drinking water source has been of great concern because of its toxicity and carcinogenicity. Prolonged exposure of arsenic is associated with cancer of the skin, lungs, urinary tracks, kidney and liver (Zhang et al. 2016). Many countries in Asia and Europe still suffer of elevated arsenic concentration in ground water used for human consumptions. These households are most of villages and not connected to the decentralized water supply system (Casentini et al. 2016). For drinking water needs at small scale, it is essential to remove arsenic below the drinking water limit 10 $\mu\text{g/L}$. Various treatment methods have been

used to remove arsenic from aqueous system including precipitation, adsorption, ion-exchange and reverse osmosis (Li et al. 2011). Adsorption by activated carbon is still the best available technique for removal of arsenic except, that its manufacturing cost is quite high (Yao et al. 2014) and also the application of activated carbon powder in water treatment process and reuse the tiny particles (Yao et al. 2014). Therefore, the adsorbent surface may be tailored to enhance the removal of specific environmental contaminants (Heskins and Karanfil 2002). A number of researchers have shown that the tendency of arsenic to strongly bind to iron oxides/hydroxides at all concentrations (Curdy et al. 2008; Dixit and Hering 2003; Mohan and Pittman 2007) and iron can be tailored with any adsorbent. In the present study, it is examined that activated carbon prepared from a cheaply available plant *Prosopis spicigera* L. wood (PsLw) and its iron oxide composite have been used to remove arsenic from aqueous system.

✉ Ramasubbu DhanaRamalakshmi
dhana.ram11@gmail.com

¹ Manonmaniam Sundaranar University,
Abishekapatti, Tirunelveli 627 012, Tamil Nadu, India

² Department of Chemistry, Sri K.G.S. Arts College,
Srivaikuntam, Thoothukudi 628 619, Tamil Nadu, India

³ Department of Chemistry, St. Xavier's College
(Autonomous), Palayamkottai, Tirunelveli 627 002,
Tamil Nadu, India

Materials and methods

PsLw carbon–iron oxide composite preparation

PsLw plant material used in the present work was collected from the dry land area of Palayamkottai in Tirunelveli district, Tamilnadu state, India. The branch and roots of the plant were cut into pieces and piled up on a firing hearth. Before firing, the heaped wood pieces were enclosed by fresh plantain pith and the whole mass was covered and plastered with layers of wet clay. This arrangement prevented the direct entry of air into wood pieces and hence burning of wood and thereby turning into ash is prohibited. After 48 h of continuous firing and subsequent natural cooling, the activated carbon was obtained. After removing the non-carbonaceous materials the carbon was isolated, crushed and sieved to 75 micron particles. The composite adsorbent was prepared using the slightly modified literature procedure (Schwarz et al. 1984; Chang et al. 2010). 20.0 g of PsLw carbon was suspended in 400 ml of FeCl_3 (7.8 g, 28 mmol) and FeSO_4 (3.9 g, 14 mmol) at 70 °C. The above solution was stirred well using a magnetic stirrer for 3 h. Sodium hydroxide solution (100 ml, 5 mol/L) was added drop wise to precipitate the iron oxides. Again the stirring was continued for another 2 h at 70 °C. Later the solid material was separated, washed with de-ionised water until the washings become neutral. Further the washings were tested for iron with 1, 10-Phenanthroline for reddish colour or precipitates. The final product was dried in an air oven at 100 °C for 8 h and finally stored in air tight containers.

Characterisation of the adsorbent

The surface morphology of PsLw carbon–iron oxide composite was studied on Jeol, JSM 6390, Oxford instruments, UK, SEM. FTIR spectroscopy was carried out on JASCO FT/IR-4700 type A to analyse the surface functional groups. The zero point charge of the adsorbent was determined by potentiometric titration (Schwarz et al. 1984). The surface area of the adsorbent was determined by methylene blue method (Potgiefer 1991) and Nitrogen BET adsorption method.

Batch equilibrium studies

Standard arsenic(III) stock solution of 1000 mg/L was prepared by dissolving 1.32 g of arsenic(III) oxide with 1000 mL of deionized water. This stock solution was utilised for batch studies. Batch equilibrium studies were carried out for adsorption of arsenic on PsLw carbon–iron oxide composite. The effect of pH, initial concentration, contact

time, in the presence of other ions and solution temperature of the adsorbate solution on PsLw carbon–iron oxide composite were studied. The sample solutions were analysed at particular time intervals using the literature procedure (Jeffery et al. 1989; Roy et al. 2013) for higher concentrations. Samples from the column study were analysed using Atomic Absorption Spectrophotometer (Shimadzu, AA-6300). The lower detectable limit of the spectrophotometric method is 0.25 $\mu\text{g/mL}$. Each sample was analysed twice and the results are reproducible within $\pm 1\%$ error limit. Further the results obtained from the spectrophotometric method are comparable with the AAS method (lower detectable limit is 0.01 $\mu\text{g/mL}$) and the deviation is $\pm 3\%$ only, which is within the error limit in order to make use of this process for large scale treatment and small scale for potable water.

The amount of adsorbate adsorbed at equilibrium, q_e (mg/g) was calculated as

$$q_e = (C_0 - C_e)V/W \quad (1)$$

where C_0 and C_e (mg/L) are the initial and equilibrium concentration of adsorbate, respectively. V is the volume of the solution (L) and W is the mass of adsorbent (g).

Adsorption isotherm models

The Langmuir (theoretical isotherm) and Freundlich (empirical) models were used to investigate the isotherm data and their linear form, are given in Eqs. (2) and (3), where, C_f and q are the free and sorbed concentration of arsenic species, respectively, at equilibrium; Q_0 and b are the Langmuir constants representing the sorption capacity and energy, respectively. K_f and n are the Freundlich constants related to the adsorption capacity and intensity, respectively.

$$C_f/q = 1/Q_0b + C_f/Q_0 \quad (2)$$

$$\log q = \log K_f + 1/n \log C_f \quad (3)$$

Adsorption kinetics

The kinetic data of arsenic adsorption onto the PsLw carbon–iron oxide composite are analysed using the pseudo-first-order (Eq. 4) and the pseudo-second-order models (Eq. 5), where q_e and q are the quantity of arsenic adsorbed at equilibrium and at time 't' and k_1 is the adsorption rate constant; k_2 is the reaction rate constant and ($q_e(\text{cal})$) is a numerically determined parameter.

$$\ln (q_e - q) = \ln q_e - k_1 t \quad (4)$$

$$t/q_t = 1/k_2q_e^2 + t/q_e \tag{5}$$

Column study

The experimental unit consists of a glass column of 48 cm height by 3.5 cm diameter packed with 5.0 g of PsLw carbon–iron oxide composite. The column was fitted with cotton screens to separate the adsorbent from the top and bottom stoppers. The arsenic solution was drawn into the column from a height of 1 m. Elutents were collected at regular interval of time and analysed. The data were analysed using Thomas model (Thomas 1948) which is given in Eq. (6)

$$\log (C_0/C_e - 1) = kq_0M/Q - kC_0V/Q \tag{6}$$

where C_0 and C_e are the influent and effluent arsenic concentrations (mg/L), respectively, k is the Thomas rate constant (mL/min/mg), q_0 is the maximum solid phase concentration of solute (mg/g), M is the mass of the adsorbent (g), Q is the influent flow rate (mL/min) and V is the through put volume (mL/min).

Results and discussion

Characterisation of the adsorbent

The physico-chemical properties of PsLw carbon–iron oxide composite are listed in Table 1.

Surface area and pore volume were determined using BET method for PsLw carbon are 120.91 m²/g and 0.9728 cm³, respectively. For PsLw carbon–iron oxide composite the surface area and pore volume are 98.61 m²/g and 0.662 cm³. Surface area as determined by methylene blue method is 50.54 m²/g and 64.53 m²/g, respectively, for PsLw carbon and iron oxide decorated carbon. The pH_{zpc}

Table 1 Physico-chemical properties of PsLw carbon–iron oxide composite

Parameters	PsLw carbon–iron oxide composite
pH	7.1
Moisture Content % (W/W)	0.0123
Surface area (m ² /g) (Nitrogen BET adsorption method)	98.61
Surface area (m ² /g) (Methylene blue dye adsorption method)	64.53
pH_{zpc}	8.22
Bulk density (g/mL)	0.4137
Particle density (g/mL)	1.3790

values are found to be 6.98 and 8.22 for the carbon and the composite, respectively.

Effect of pH

Arsenate species and the surface charge of the adsorbent in aqueous solution are pH dependent, which make pH be one of the most important factors affecting arsenate adsorption on to the adsorbent in the liquid phase (Chang et al. 2010). The effect of pH on arsenic adsorption onto PsLw carbon–iron oxide composite is shown in Fig. 1. It is seen that the sorption of arsenic is most appreciable in the pH range 1.0–3.0 and decreases with increase in pH. The adsorption capacity is 99.7 mg/g in this pH range and at pH=6.0 the adsorption capacity is 77.7 mg/g. In order to apply this process to practical application the studies are performed at pH=6.0. Arsenic species in aqueous medium exist mainly as H₃AsO₃ at pH is less than 2.2; H₂AsO₃⁻ at pH between 2.2 and 6.98; HAsO₃²⁻ at pH between 6.98 and 11.5, and AsO₄³⁻ at pH above 11.5 (Chang et al. 2010). It is well known that the surface of the adsorbents are positively charged when the pH of the solution is less than pH_{zpc} and negatively charged when the pH is above pH_{zpc} . In the present system the pH_{zpc} of the adsorbent is 8.22 and the surface of PsLw carbon–iron oxide composite is positively charged below pH=8.22. Therefore at pH=6.0, the sorption of arsenic may be due to electrostatic interaction between predominant arsenic species H₂AsO₃⁻ with more positively charged PsLw carbon–iron oxide composite (Te et al. 2015).

Effect of contact time and initial concentration

The effect of contact time and initial concentration on PsLw carbon–iron oxide composite is shown in Fig. 2,

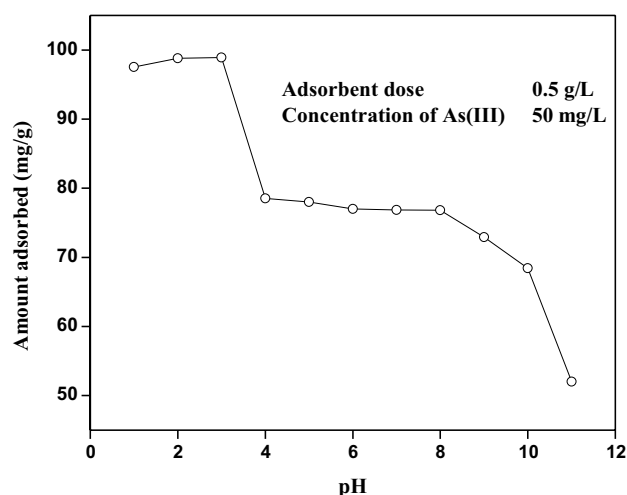


Fig. 1 Effect of pH

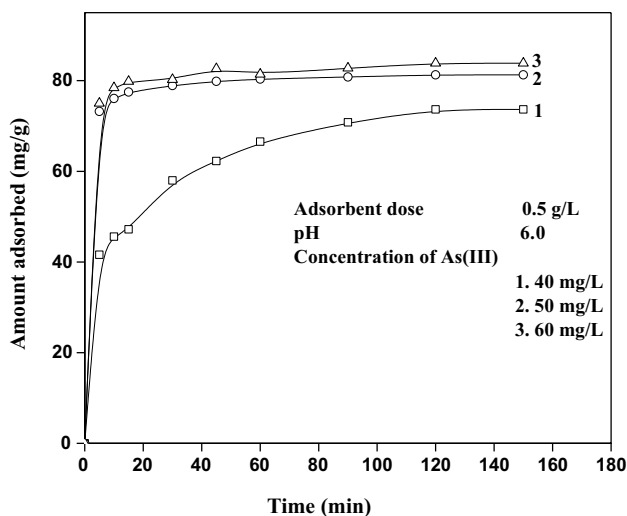


Fig. 2 Effect of contact time and initial concentration

which clearly indicates the adsorption is maximum within the first 60 min of agitation time and reached equilibrium after 160 min. The maximum adsorption capacities of arsenic on PsLw carbon–iron oxide composite are 73.66, 81.28, 83.84 mg/g for the initial concentrations 40, 50 and 60 mg/L, respectively. The higher adsorption capacity at high initial concentrations may be due to stronger driving force of the concentration gradient (Li et al. 2009; Mahmoud et al. 2012).

Effect of temperature

The effect of solution temperature on adsorption of arsenic onto PsLw carbon–iron oxide composite is depicted in Fig. 3. The maximum adsorption of arsenic on PsLw

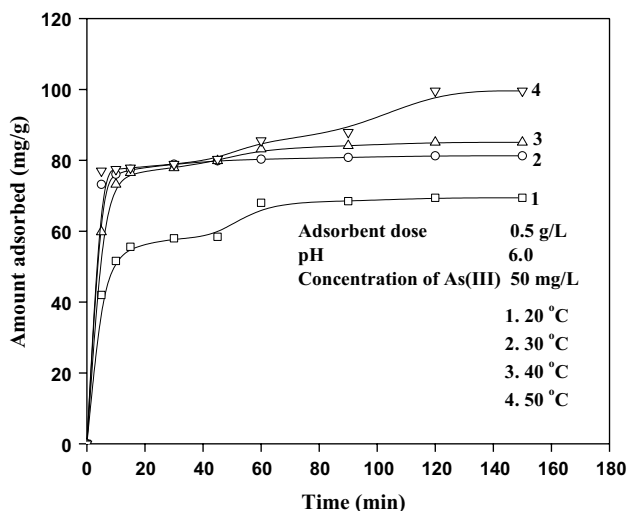


Fig. 3 Effect of temperature

carbon–iron oxide composite are 69.42, 81.28, 85.08 and 99.6 mg/g at 20, 30, 40 and 50 °C, respectively. The adsorption capacity increases with increase in temperature. The increase in uptake of arsenic species with temperature may be due to the elevated intraparticle diffusion, since diffusion is an endothermic process (Banerjee et al. 2008).

Effect of adsorption of arsenic in the presence of other ions

Batch study was carried out in the presence of other ions such as carbonate, nitrate, chloride and sulphate of concentration 0.001 M each. Figure 4 shows the adsorption capacity increases with time and equilibrium is reached at 140 min for an initial concentration of 50 mg/L. The maximum adsorption capacity of arsenic was found to be 49.6 mg/g which is lower than the adsorption capacity of arsenic in the absence of other ions. This may be due to the competition between other ions with arsenic species for the same number of adsorption sites. This application of the present study is helpful to practical purposes.

Adsorption isotherm

The isotherm variables for the Langmuir and Freundlich isotherms were determined from Eqs. (2) and (3). The linear plots of C_i/q against C_i in Langmuir model for the adsorption of arsenic on PsLw carbon–iron oxide composite at different concentrations and temperatures are shown in Fig. 5. From the slope and intercept of the plot the Langmuir parameters can be calculated. The Freundlich isotherm variables were determined by plotting $\log q_e$ versus $\log C_e$ (The figures are not given). For the PsLw

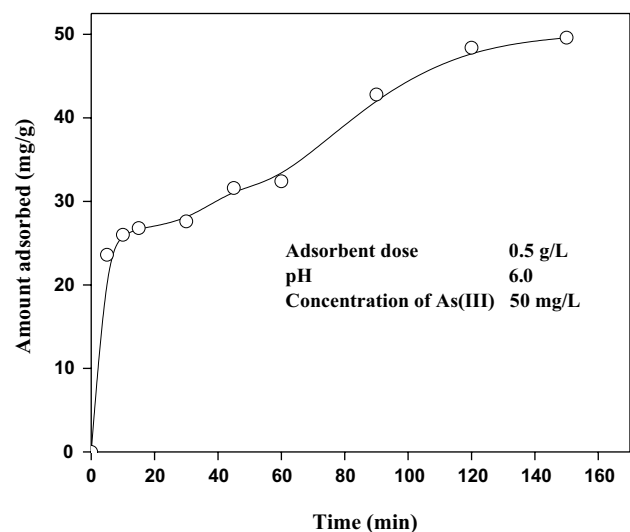


Fig. 4 Effect of As(III) in the presence of other ions

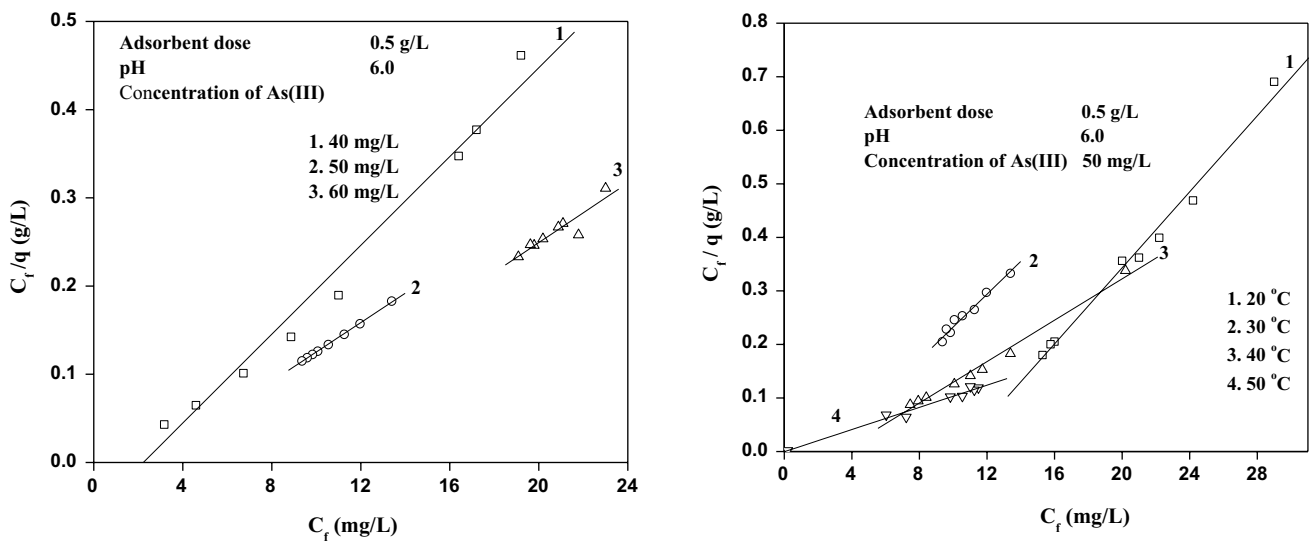


Fig. 5 Langmuir isotherm for As(III) adsorption at different concentrations and temperatures

Table 2 Langmuir isotherm constants at different concentrations and temperatures

C_0 (mg/L)	Temp (°C)	Q_0 (mg/g)	b (L/mg)	R_L	R
40	30	53.68	0.45	0.0526	0.9906
50	30	59.24	0.4024	0.0473	0.9995
60	30	59.17	0.3905	0.0409	0.9902
50	20	54.15	0.1123	0.1512	0.9863
50	30	59.24	0.4024	0.0473	0.9995
50	40	68.81	0.5025	0.0383	0.9942
50	50	79.36	0.7876	0.0248	0.9949

carbon–iron oxide composite the Langmuir model gives a good fit with the experimental data and the results are given in Table 2. However, the Freundlich model does not provide a good correlation with the experimental data. The nature of adsorption isotherm can be investigated by the dimensionless separation factor, R_L , which is given as

$$R_L = 1 / (1 + bC_0) \tag{7}$$

where C_0 is the initial concentration (mg/L) of arsenic.

The separation factor $R_L = 0$ for irreversible; $0 < R_L < 1$ for favourable; $R_L = 1$ for linear and $R_L > 1$ for unfavourable. The separation factor R_L is found to be < 1 which indicates favourable adsorption process. The decrease in R_L value with increase in the initial concentration and temperature indicates that the adsorption process is more

favourable at high concentrations and high temperatures (Mi-Hwa et al. 2010).

Batch kinetic studies

The rate constant (k_1) and the equilibrium adsorbed capacity ($q_e(\text{cal})$) of pseudo-first-order models were determined from the linear plot of $\log(q_e - q)$ versus time at different concentration of ions and temperature using Eq. (4). The rate constant k_2 and ($q_e(\text{cal})$) of pseudo-second-order models were determined from the linear plot of t/q_t against time at different concentrations and temperatures using Eq. (5) and the plots are displayed in Fig. 6.

The kinetic parameters are given in Table 3. The closeness of experimental ($q_e(\text{exp})$) adsorption capacity value of pseudo-second-order with the calculated equilibrium capacity ($q_e(\text{cal})$) shows the arsenic adsorption on PsLw carbon–iron oxide composite follows pseudo-second-order kinetics.

Thermodynamic parameters

The equilibrium constant (k), free energy change (ΔG°), enthalpy change (ΔH°), and entropy change (ΔS°) for arsenic adsorption are determined at different temperatures using Eqs. (8), (9) and (10)

$$\Delta G^\circ = -RT \ln k \tag{8}$$

$$\ln k = \left(\Delta S^\circ / R \right) - \left(\Delta H^\circ / RT \right) \tag{9}$$

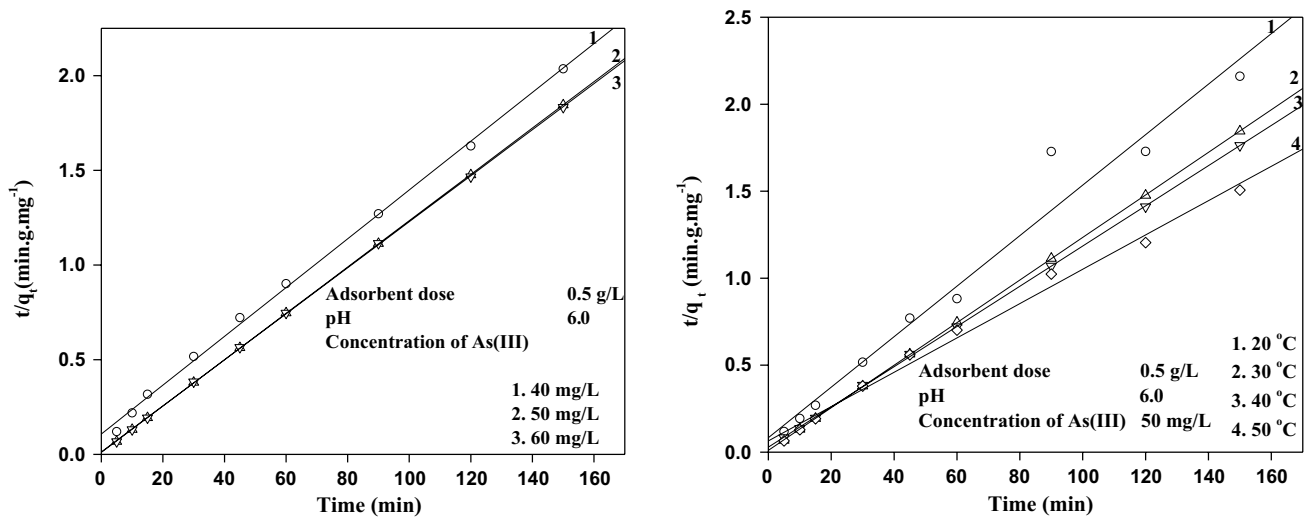


Fig. 6 Pseudo-second-order plot at different concentrations and temperatures

Table 3 Comparison of pseudo-first-order and pseudo-second-order kinetic parameters

C ₀ (mg/L)	Temp (°C)	q _e (exp) (mg/g)	Pseudo-first order			Pseudo-second order		
			k ₁ (min ⁻¹)	q _e cal (mg/g)	R ²	k ₂ (g/mg/min)	q _e (cal) (mg/g)	R ²
40	30	73.66	0.0286	38.35	0.9970	0.0015	77.52	0.9982
50	30	81.28	0.0320	07.02	0.9684	0.0140	81.98	0.9998
60	30	83.83	0.0226	06.77	0.9370	0.0113	82.24	0.9998
50	20	69.42	0.0398	31.24	0.8844	0.0025	68.96	0.9688
50	30	81.28	0.0320	07.02	0.9684	0.0140	81.98	0.9998
50	40	85.08	0.0350	20.07	0.9415	0.0047	86.21	0.9998
50	50	99.60	0.0081	24.67	0.9306	0.0015	101.01	0.9916

Table 4 Thermodynamic parameters

Temperature (K)	-ΔG° (kJ/mol)	ΔH° (kJ/mol)	ΔS° (J/mol K)
293	43.31	364.15	1.39
303	63.99		1.41
313	66.88		1.38
323	88.89		1.40

Table 5 Pore diffusion constant

C ₀ (mg/L)	T (°C)	Intra particle diffusion (k _i) (mg/g/min ^{1/2})	β _L (cm/s)
40	30	1.0354	–
50	30	1.6893	–
60	30	1.8084	–
50	20	1.4099	0.0006
50	30	1.6323	0.0031
50	40	2.4385	0.0075
50	50	3.5243	0.0104

$$\Delta G^\circ = \Delta H^\circ - T\Delta S^\circ \tag{10}$$

where *T* is the temperature (K) and *R* is the gas constant (8.314 J/mol K). Δ*H*[°] and Δ*S*[°] value can be calculated from the slope and the intercept. The thermodynamic parameters are listed in Table 4.

The negative value of Δ*G*[°] indicates that the adsorption of arsenic on PsLw carbon–iron oxide composite is a spontaneous process. The positive value of Δ*H*[°] shows that the adsorption process is endothermic. The Δ*S*[°] value increases with temperature, which indicates the randomness

of adsorption of arsenic on adsorbent surface. From thermodynamic parameters, the adsorption process is found to be spontaneous and endothermic in nature (Jain and Agarwal 2017; Banerjee et al. 2008).

Pore diffusion and mass transfer

In sorption process, the ions are likely to diffuse into the interior of the porous adsorbent. In the present system also, this is a likely process. The plots of square root of contact time ($t^{1/2}$) against adsorption capacity (q) at different concentrations and temperatures are parabolic but linear for some contact times at the initial stage. Moreover they do not pass through origin. This pattern obviously represents that intraparticle diffusion contributes significantly to the rate process at initial stage. The slope of the linear portion of the plots (Figures not shown) has been reported in rate parameter (pore diffusion constants) and is given in Table 5.

The external mass transfer of adsorbate towards the sorbent was studied using Eq. (11) proposed by McKay et al. (1981) where C_0 (mg/L) is the initial adsorbate concentration and C_t (mg/L) is the adsorbate concentration after time t , ' m ' is the mass of adsorbent per unit volume of particle free solution (g/L), k (L/g) is the product of Langmuir constants Q_0 and b , β_L (cm/s) is the mass transfer coefficient while S_s is the outer surface area of adsorbent per unit volume of particle free slurry (cm^{-1}). The values of ' m ' and ' S_s ' were calculated using the relations (12) and (13).

$$\ln \left[\left(\frac{C_t}{C_0} \right) - \frac{1}{(1 + mk)} \right] = \left[\frac{(1 + mk)}{mk} \beta_L S_s \right] t + \left[\frac{mk}{(1 + mk)} \right] \quad (11)$$

$$m = W/v \quad (12)$$

$$S_s = 6m/(1 - \epsilon_p) d_p \rho_p \quad (13)$$

where W is the weight of adsorbent (g), ' v ' is the volume of particle free adsorbate solution (L), d_p is the particle diameter (cm), ρ_p is the density of adsorbent (g/cm^3) and ϵ_p is the porosity of adsorbent particle. The plot of $\ln \left[\left(\frac{C_t}{C_0} \right) - \frac{1}{(1 + mk)} \right]$ against t is a straight line (Figure not shown). From the slope and intercept of the plot, the mass transfer coefficient β_L was calculated and listed in Table 5. The mass transfer coefficient increases with increase in temperature.

Adsorption mechanism

From the pore diffusion and mass transfer studies, it is learnt that As(III) species get adsorbed into the pores by surface adsorption and external mass transfer process. In addition to this, As(III) gets adsorbed onto the adsorbent through complex formation with ferric oxy/hydroxides (Li et al. 2011). Under the experimental conditions, As(III) species exist as H_3AsO_3 , H_2AsO_3^- and HAsO_3^{2-} and surface complex reaction with the adsorbent may be represented by the following equations.

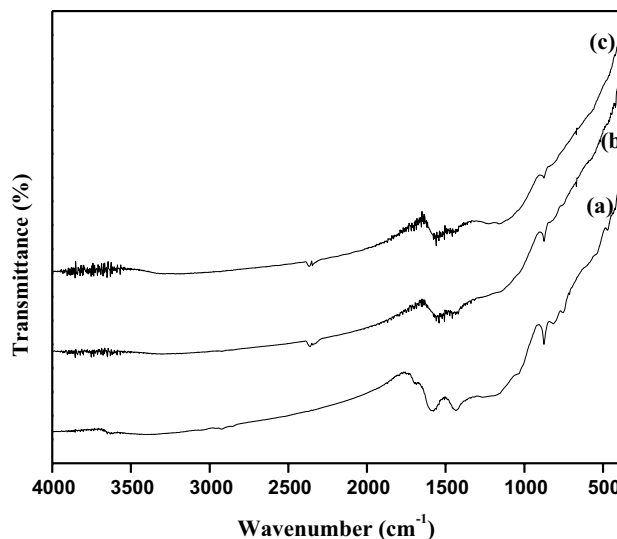
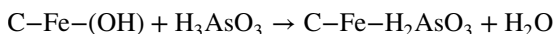
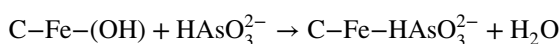
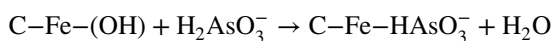


Fig. 7 FTIR spectrum of **a** pure PsLw carbon **b** PsLw carbon-iron oxide composite **c** As loaded PsLw carbon-iron oxide composite



The complex formation and mass transfer are evident from the IR spectral and SEM studies. The FTIR spectra of pure PsLw carbon, PsLw carbon-iron oxide composite and As(III) loaded PsLw carbon-iron oxide composite are illustrated in Fig. 7a-c. Three weakly intense peaks at 1613 cm^{-1} (due to ketone moiety), 1423 cm^{-1} (O-H in plane bending) and 961 cm^{-1} (C-O stretching) were displayed in the PsLw carbon (Fig. 7a).

The peaks at 1613 cm^{-1} and 1423 cm^{-1} have been broadened and the peak at 961 cm^{-1} disappeared shows reaction between carbon surface and iron oxide. In the As(III) loaded adsorbent the broadened peaks are unaffected but a new weak intense peak appears at 784 cm^{-1} . This may be due to As(III)-O bond (Gupta et al. 2009). The SEM image of pure PsLw carbon (Fig. 8a) reveals that, there are irregularly shaped and sized carbon particles with well-developed porous structure which are aggregated to give larger size particles in the iron oxide decorated composite (Fig. 8b). It is also observed that the composite consists of brighter patches of iron oxide on the darker surface of the PsLw carbon. After sorption of As(III) the particles are further agglomerated with less number of brighter patches of iron oxide (Fig. 8c). Thus the As(III) adsorption onto PsLw carbon-iron oxide composite involves surface adsorption, pore diffusion, external mass transfer and complex formation.

Fig. 8 SEM images of **a** pure PsLw carbon **b** PsLw carbon–iron oxide composite **c** As(III) loaded PsLw carbon–iron oxide composite

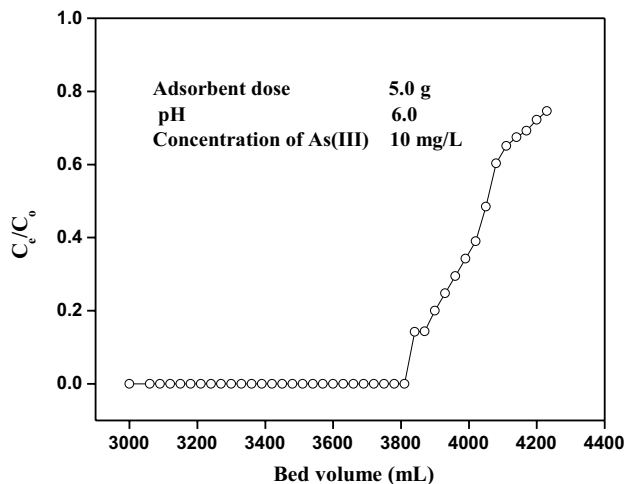
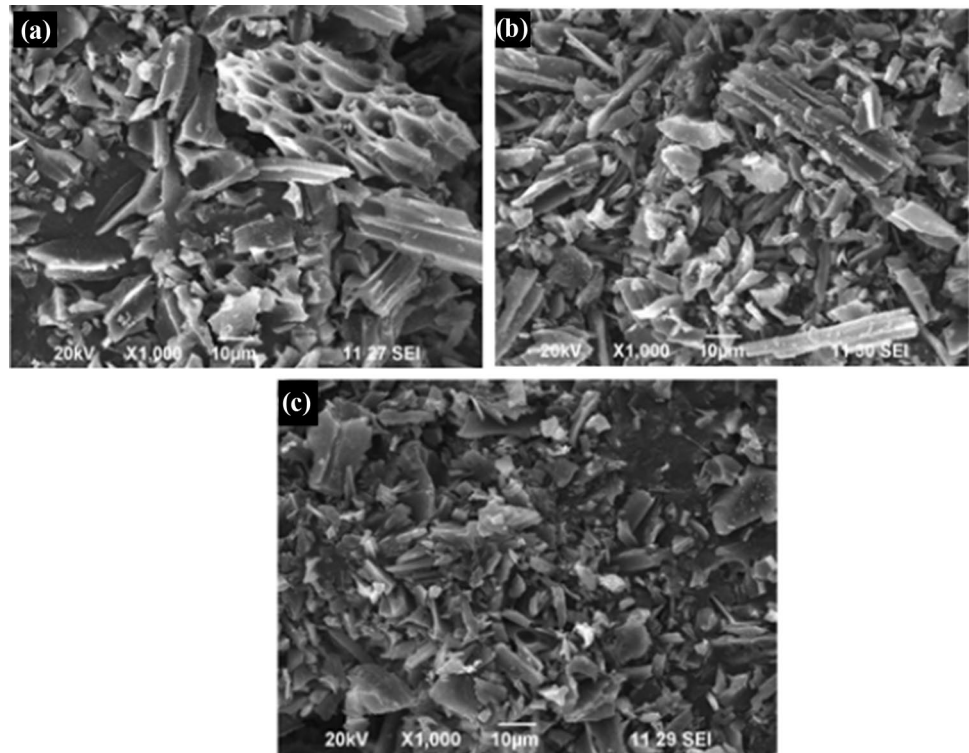


Fig. 9 Breakthrough curve of column study of arsenic removal

Column study

The breakthrough curve for sorption of arsenic on PsLw carbon–iron oxide is shown in Fig. 9. Effluent arsenic ion concentration was found to be zero for first 3840 ml (128 bed volumes) for an initial concentration of 10 mg/L; approximately 7.1 mg of arsenic is retained for 150 ml (5 bed volumes); 2.5 mg for another 300 ml (10 bed volumes) and the retention of arsenic by the column gradually declines as the effluent volume increases. The Thomas rate constant k and

the maximum solid phase concentration of arsenic q_0 values are computed from the slope and intercepts of the linear plot of $\log(C_0/C_e - 1)$ versus V are found to be 1.065 mL/min/mg and 0.4503 mg/g, respectively. When the column was saturated with arsenic ion, it was eluted with 0.1 M NaOH. These column analysis data are useful and provide a rough estimate of arsenic sorption in practical macro-level column treatment.

Desorption studies

For studying the regeneration of PsLw carbon–iron oxide composite, the adsorption and desorption processes were repeated. The effect of pH on the sorption of the adsorbent shows the adsorption capacity decreases with increasing pH. Therefore, the desorption was carried out with 0.1 M NaOH. The desorption of arsenic was 90%. But iron was not leached out since the desorbed solution does not give any colouration with 1, 10-Phenanthroline. The adsorption–desorption studies were carried out for three cycles and the adsorption capacities are 86% and 81% for the second and third cycle.

Comparison with other adsorbents

The comparative study of different adsorbents for the removal of arsenic is given in Table 6. The low cost PsLw carbon–iron oxide composite has remarkable efficiency for the removal of arsenic compared with other adsorbents. The variation of

Table 6 Adsorption capacity of different adsorbents

Adsorbent	Adsorption capacity, q (mg/g)	References
Iron oxide coated multiwall carbon nanotubes	1.723	Ntim and Mitra (2011)
Bagasse fly ash	0.021	Ali et al. (2014)
Spent grains	3.0	Yunnen et al. (2017)
Bacterial iron oxide nanowires	4.99	Andjelkovic et al. (2017)
Fe-FeS ₂ ball milling	101.123	Min et al. (2017)
Goethite-P(AAm) (polyacrylamide) composite	1.22	Ramirez-Muniz et al. (2018)
Pure Akaganeite (β -FeO(OH))	148.7	Polowczyk et al. (2018)
Aminatedpoly(glycidyl methacrylate)	13.5	Park et al. (2019)
Chitosan magnetic graphene oxide	45.0	Sherlala et al. (2019)
TiO ₂	50.5	Zhou et al. (2019)
Activated charcoal coated Zr–Mn nanocomposite	132.28	Yin et al. (2019)
PsLw carbon–iron oxide composite	83.84	Present study

amount of adsorption is due to the individual characteristics of adsorbent, extent of adsorbent surface and initial concentration.

Conclusion

The work examined the adsorption of arsenic from aqueous solution using the low cost PsLw carbon–iron oxide composite. The iron modified adsorbent yields interesting results. Batch adsorption studies indicated the sorption process fit Langmuir isotherm with maximum adsorption capacity 83.84 mg/g at 30 °C. The kinetic data denotes the sorption follows pseudo-second order. From the thermodynamic parameters, the process was found to be spontaneous and endothermic in nature. For industrial application, the effective removal of arsenic using PsLw carbon–iron oxide composite was made by Thomas model. The external mass transfer of adsorbate accompanies with slow rate of intra particle diffusion. All the parameters exhibit major role of PsLw carbon–iron oxide composite for the removal of arsenic from aqueous solution. Thus, it is concluded that the low cost PsLw carbon–iron oxide composite have an excellent potential for the removal of arsenic for potable and industrial applications.

Acknowledgements We acknowledge the administration of Sri K.G.S Arts College, Srivaikuntam, St. Xavier's College (Autonomous), Palayamkottai and Rani Anna Government College for Women, Tirunelveli for all the laboratory studies.

Funding The authors declare that they have no known competing financial interests or personal relationships that could have appeared to influence the work reported in this paper.

Compliance with ethical standards

Conflict of interest The authors declare no competing financial support.

Open Access This article is licensed under a Creative Commons Attribution 4.0 International License, which permits use, sharing, adaptation, distribution and reproduction in any medium or format, as long as you give appropriate credit to the original author(s) and the source, provide a link to the Creative Commons licence, and indicate if changes were made. The images or other third party material in this article are included in the article's Creative Commons licence, unless indicated otherwise in a credit line to the material. If material is not included in the article's Creative Commons licence and your intended use is not permitted by statutory regulation or exceeds the permitted use, you will need to obtain permission directly from the copyright holder. To view a copy of this licence, visit <http://creativecommons.org/licenses/by/4.0/>.

References

- Ali I, Al-Othman ZA, Alwarthan A, Asim M, Khan TA (2014) Removal of arsenic species from water by batch and column operations on bagasse fly ash. *Environ Sci Pollut Res* 21:3218–3229
- Andjelkovic I, Azari S, Erkelens M, Forward P, Lambert MF, Losic D (2017) Bacterial iron-oxide nanowires from biofilm waste as a new adsorbent for the removal of arsenic from water. *RSC Adv* 7:3941–3948
- Banerjee K, Amy GL, Prevost M, Nour S, Jekel M, Gallagher PM, Blumenschein CD (2008) Kinetic and thermodynamic aspects of adsorption of arsenic onto granular ferric hydroxide (GFH). *Water Res* 42:3371–3378

- Casentini B, Falcione FT, Amalfitano S, Fazi S, Rossetti S (2016) Arsenic removal by discontinuous ZVI two steps system for drinking water production at household scale. *Water Res* 106:135–145
- Chang Q, Lin W, Ying WC (2010) Preparation of iron-impregnated granular activated carbon for arsenic removal from drinking water. *J Hazard Mater* 184(1–3):515–522
- Curdy AB, Hopkinson L, Whitby RLD (2008) Use of iron-based technologies in contaminated land and groundwater remediation: a review. *Sci Total Environ* 400(1–3):42–51
- Dixit S, Hering J (2003) Comparison of arsenic(V) and arsenic(III) sorption onto iron oxide minerals: implications for arsenic mobility. *Environ Sci Technol* 37(18):4182–4189
- Gupta A, Chauhan VS, Sankararamkrishnan N (2009) Preparation and Evaluation of iron- chitosan composites for removal of As(III) and As(V) from arsenic contaminated real life ground water. *Water Res* 43:3862–3870
- Heskins JS, Karanfil T (2002) Removal and sequestration of iodide using silver-impregnated activated carbon. *Environ Sci Technol* 36:784–789
- Jain A, Agarwal M (2017) Kinetic equilibrium and thermodynamic study of arsenic removal from water using alumina supported iron nano particles. *J Water Process Eng* 19:51–59
- Jeffery GH, Bassett J, Mendham J, Denny RC (1989) Vogel's textbook of quantitative chemical analysis. Longmann Scientific & Technical, England
- Li K, Zheng Z, Huang X, Zho G, Feng J, Zhang J (2009) Equilibrium, kinetic and thermodynamic studies on the adsorption of 2-nitroaniline onto activated carbon prepared from cotton stalk fibre. *J Hazard Mater* 166:213–220
- Li Z, Jean JS, Jiang WT, Chang PH, Chen CJ, Liao L (2011) Removal of arsenic from water using Fe-exchanged natural zeolite. *J Hazard Mater* 187:318–323
- Mahmoud DK, Salleh MA, Wan WA, Abdul Karim A, Idris A, Zainal Abidin Z (2012) Batch adsorption of basic dye using acid treated kenaf fiber char: equilibrium, kinetic and thermodynamic studies. *J Chem Eng* 181–182:449–457
- Mckay G, Otterburn MS, Sweeney AG (1981) Surface mass transfer process during color removal from effluent using silica. *Water Res* 15(3):327–331
- Mi-Hwa B, Ijagbemi BCO, Se-Jin O, Kim DS (2010) Removal of malachite green from aqueous solution using degreased coffee bean. *J Hazard Mater* 176(1–3):820–828
- Min X, Li Y, Ke Y, Shi M, Chai L (2017) Fe–FeS₂ adsorbent prepared with iron powder and pyrite by facile ball milling and its application for arsenic removal. *Water Sci Technol* 76(1):192–200
- Mohan D, Pittman CU (2007) Arsenic removal from water/wastewater using adsorbents—a critical review. *J Hazard Mater* 142(1–2):1–53
- Ntim SA, Mitra S (2011) Removal of trace arsenic to meet drinking water standards using iron oxide coated multiwall carbon nanotubes. *J Chem Eng Data* 56:2077–2083
- Park H, Nguye DC, Na CK, Bui TH, Sun KH (2019) Removal of arsenic from aqueous solutions using aminated poly(glycidyl methacrylate). *J Water Supply Res Technol Aqua* 68(4):243–252
- Polowczyk I, Cyganowski P, Ulatowska J, Sawiński W, Bastrzyk A (2018) Synthetic iron oxides for adsorptive removal of arsenic. *Water Air Soil Pollut* 229:203
- Potgiefer JH (1991) Adsorption of methylene blue on activated carbon: an experiment illustrating both the Langmuir and Freundlich isotherms. *J Chem Edu* 68(4):349
- Ramirez-Muniz K, Perez-Rodriguez F, Rangel-Mendez R (2018) Adsorption of arsenic onto an environmental friendly goethite-polyacrylamide composite. *J Mol Liq* 264:253–260
- Roy P, Mondal NK, Bhattacharya S, Das B, Das K (2013) Removal of arsenic(III) and arsenic(V) on chemically modified low-cost adsorbent: batch and column operations. *Appl Water Sci* 3:293–309
- Schwarz JA, Driscoll CT, Bharot AK (1984) The zero point of charge of silica-alumina oxide suspensions. *J Colloid Interface Sci* 97(1):55–61
- Sherlala AIA, Raman AA, Bello MM, Buthiyappan A (2019) Adsorption of arsenic aqueous solution using magnetic graphene oxide. *J Environ Manag* 246:547–556
- Te B, Wichitsathian B, Yossapol C (2015) Modification of natural common clays as low cost adsorbents for arsenate adsorption. *Int J Environ Sci Dev* 6(11):799–804
- Thomas HC (1948) Chromatography: a problem in kinetics. *Ann N Y Acad Sci* 49:161–182
- Yao S, Liu Z, Shi Z (2014) Arsenic removal from aqueous solutions by adsorption onto iron oxide/activated carbon magnetic composite. *J Environ Health Sci Eng* 12(1):58
- Yin Y, Zhou T, Luo H, Geng J, Yu W, Jiang Z (2019) Adsorption of arsenic by activated charcoal coated zirconium-manganese nanocomposite: performance and mechanism. *Colloids Surf A* 575:318–328
- Yunnen C, Ye W, Chen L, Lin G, Jinxia N, Rushan R (2017) Continuous fixed-bed column study and adsorption modeling: removal of arsenate and arsenite in aqueous solution by organic modified spent grains. *Pol J Environ Stud* 26(4):1847–1854
- Zhang L, Zhu T, Liu X, Zhang W (2016) Simultaneous oxidation and adsorption of As(III) from water by cerium modified chitosan ultrafine nanobiosorbent. *J Hazard Mater* 308:1–10
- Zhou Z, Yu Y, Ding ZM, Jing C (2019) Competitive adsorption of arsenic and fluoride on {2 0 1} TiO₂. *Appl Surf Sci* 466:425–432

Publisher's Note Springer Nature remains neutral with regard to jurisdictional claims in published maps and institutional affiliations.